Developing a Common Rail Pressure Prediction Model based on Neuro-Fuzzy networks with Local Linearized Models

Thesis submitted in partial fulfillment for
the degree of Doctor of Philosophy

University Politehnica Timişoara
Systems Engineering

Gelu-Laurenţiu Ioanaş

Coordinator: Univ. Prof. PhD. Eng. Toma-Leonida Dragomir.

Synopsis

2013

SUMMARY

1 INTRODUCTIVE CHAPTER

Modeling in detail nonliear proceses using theoretical methods and implementing the rezulted models in a numerical real time application, is time consuming and takes a lot of resources. Those aspects become critical for the automotive industry where complex systems combine interactions from mechanical, hydraulical and thermal processes. The empirical models and the corresponding identification methods are considered as an alternative to the classical approaches. The Neuro-Fuzzy networks have proven, for various complex nonlinear systems, their capabilities to supply realiable numerical models obtained from the process measurement with little knowledge about the systems [1],[2],[3],[4].

The automotive industry struggles to meet the restrictive requirements imposed by the emmisions legislation (EU6, EU7, SULEV etc.) [5][6][7] and one of the main direction of improvement is the fuel injection system. For the Piezo Common Rail injection system, the pressure in the rail plays an important role in determining the injected quantity. Since there is an inherent delay between calculation of injection parameters and the actual realization of injection, there is a necessity to have the rail pressure for the moment of injection ralization predicted at the computation instant.

In order to have a good aproximation of the pressure in the rail, a model of the nonlinear process has to be developed based on *apropri* knowledge. The accuracy of such model will be essential for realizing the required fuel quantity injection. Since the system is time variant, the model should have an adaptive behavior and adjust its parameters *on-line*. In addition, the model computation has to be done in a real time environment where additional constrains are imposed to the application such as CPU load and memory limitations.

In a simpleminded approach, the problem is twofold: *modeling* and *identification*. This PhD thesis has the purpose of treating, in a systematic manner, the two problems and determine a numerical prediction model for a wide system operating range with the capability of *on-line* adaptation of the parameters.

Chapter 2 makes a detailed presentation of the Piezo Common Rail System (PCR), providing an analytical flow – pressure model and identifying the main input variables. Chapter 3 presents the theoretical tools further used for modeling and identification, outlining the main advantages of Neuro-Fuzzy networks. Chapter 4 is dedicated to the development of the Neuro-Fuzzy model with local linear dynamic models. The proposed algorithm for input space decomposition is presented along with the model structure optimization for real time implementation.

In chapter 5 there it is presented the transformation from a Neuro-Fuzzy network model to a model based on bilinear adaptive interpolation maps fitted for implementation on a real time ECU. In the last part, a robust version of RLS adaptation algorithm is introduced. Chapter 6 presents, in all the stages, the input space partitioning algorithm and the model structure development. The results are presented is a synthetic manner, highliting the Common Rail pressure prediction model performance compared to the current solution.

Chapter 7 synthesizes the main author contributions and the main prespectives for the aplicability of the presented solution.

2 PRESSURE VARIATION MODEL IN PIEZO COMMON RAIL SYSTEMS (PCR)

New PCR grenerations have the capacity to operate in pressure ranges up to 240 MPa with a variaty of injections configurations (up to 7 injections per segment).

Fig. 1 contains a schematic representation of PCR system with 4 injectors and a 2 piston pump. The main components are: low pressure side with the electrical fuel pump (EFP) lifting the fuel from the tank and the high pressure side with the volumetric control valve (VCV) and pressure control valve (PCV), common-rail (CR). piezo injectors (INJ) and the pressure sensor (HPS). The sensors (HPS) and (TFU) send pressure and temperature information to the engien control unit (ECU) which controls all engine processes. The mechanical events are synchronized using the crankshaft position sensor (CRK).

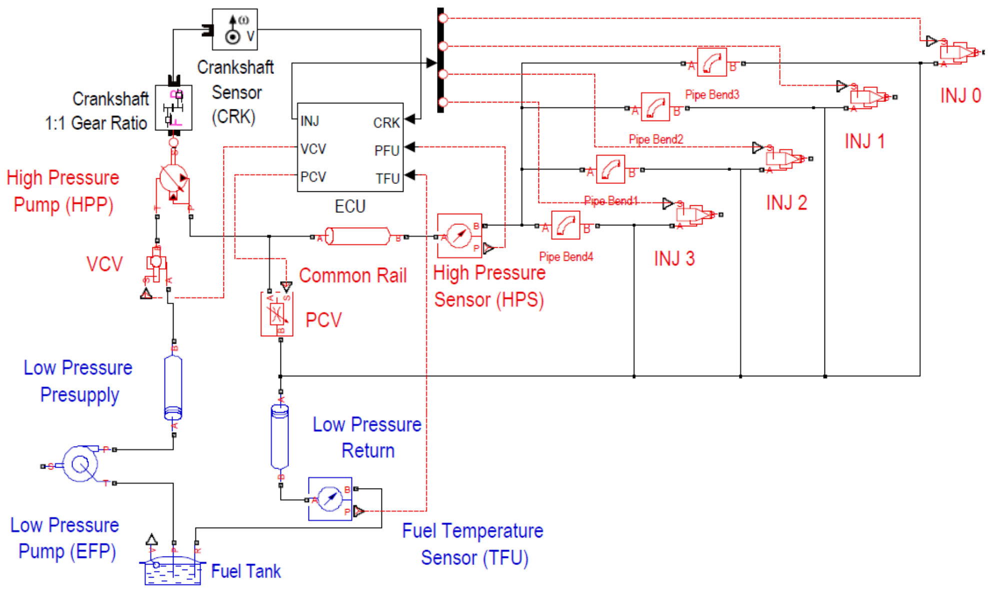

Figure 1. Piezo Common Rail System - schematics

Engine emissions management is closelly linked to combustion management which is dependent of injection realization [8]. Since the injection duration t_{INJ}, controled by the ECU, is dependent on required fuel mass and CR pressure, the injected fuel mass is directly influenced by the quality of CR pressure information.

Due to the inertial character of the measurement, computation and injection actuation, the CR pressure value used to calculate t_{INJ} has to be predicted in order to obtain the required injection quantity. Current solution uses the measured average from last segment to provide an estimation of the CR pressure value at the moment of injection. This approach can lead to deviations from setpoint for the injected fuel mass in transient conditions [15].

During the bibliografic research, studies about the common rail systems were found in several papers [10], [11], [12], [13], [14], [15], [16], [18], [19], [20], [21], [22], [23], [24], [25]. Diferent parts of the system was studied revealing the main factors influencing the pressure in the injection system. Detailed models were generated for diferent components but there was no information about a complete pressure prediction model. The subject is intensivelly covered by the autor in his published papers [17], [26], [27], [28], focusing on the particularities of the PCR system.

The fuel characteristics are depenent on the operating point defined by temperature (T) and pressure (P) [23]. The considered nonlinear mathematical model for the common-rail pressure is:

$$\frac{dP}{dt} = \frac{c^2(P,T)}{V_{rail}} \cdot \left(Q^m_{HPP}(t) - Q^m_{Leak}(t) - Q^m_{INJ}(t) - Q^m_{PCV}(t) \right). \tag{1}$$

Here: c is speed of sound, $Q^m_{HPP} = f_1(\alpha_{CRK}(t), \varphi, \psi_{VCV}(t), N(t))$ - (Q^m_{HPP} - pump mass flow rate, φ – pump mounting angle, α_{CRK} – crankshaft position, ψ_{VCV} – VCV opening [%], N – engine speed), $Q^m_{INJ} = f_2(\alpha_{CRK}(t), \alpha_{SOI}, t_{INJ}, mf_{inj})$ - (Q^m_{INJ} - injector mass flow rate, α_{SOIi} – start of injection position, mf_{inj} – injected fuel mass), $Q^m_{PCV} = f_3(\psi_{PCV}(t), P(t), T(t))$ - (Q^m_{PCV} - PCV mass flow rate, ψ_{PCV} – PCV opening [%]), $Q^m_{Leak} = f_4(P(t), T(t))$ – (Q^m_{Leak} - leakage mass flow rate). The prediction model should approximate model (1), overcoming the fact that the mass flow rates are not directly measurable.

Fig. 2 presents the CR pressure during a complete engine cycle for a 4 injector and 2 pistons pump system. All mechanical, hydraulical and computational events are presented relative to crankshapt position α_{CRK} [26].

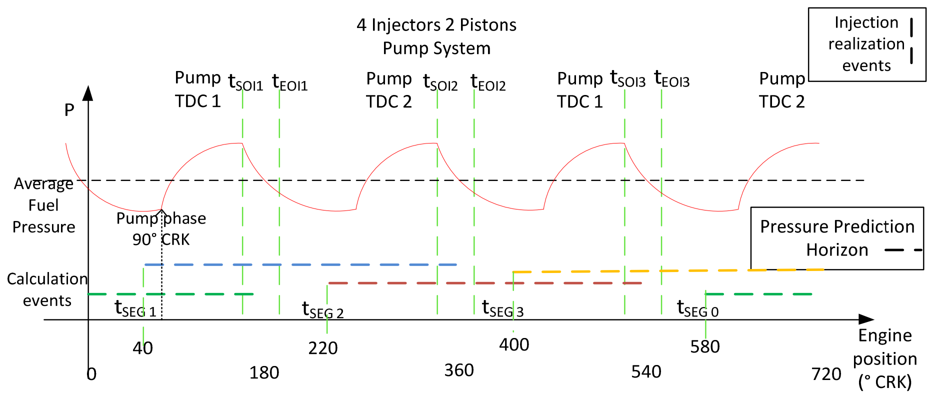

Figure 2. Inherent CR pressure variation for a complete engine cycle (720º CRK). Upper part – pressure variation with respect to pump TDC and t_{SOI}, t_{EOI}. Lower part – prediction horizon with respect to segment calculation time t_{SEG} [27].

Since the purpose of the prediction model is to accurately predict the CR pressure during injection at the moment when the injection parameters are calculated, the prediction horizon is [t_{SEGj}, $0.5(t_{SOIj+1} + t_{EOIj+1})$] of length $\tau_{INJi} = 0.5(t_{SOIj+1} + t_{EOIj+1}) - t_{SEGj}$.

An aproximate representation of the flow rates for each system component for an interval between 2 engine segments, is presented in fig. 3 [26].:

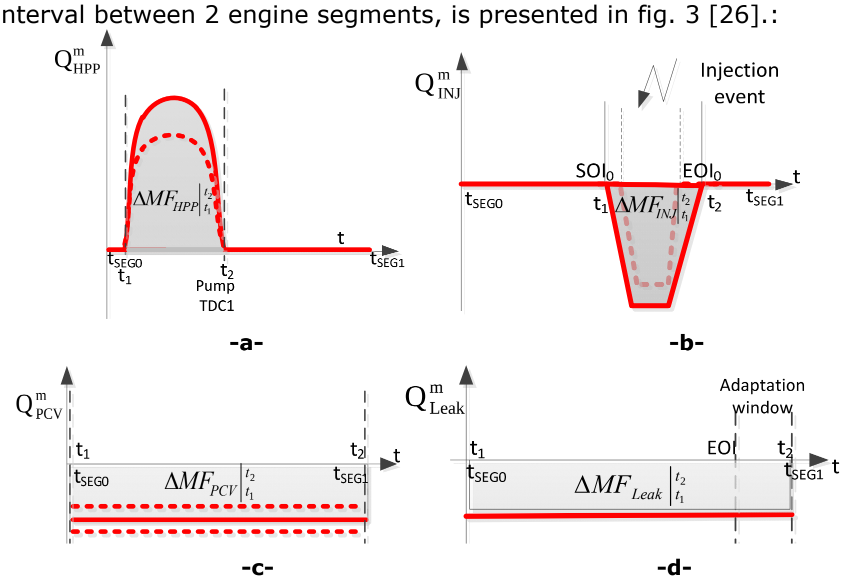

Figure 3. Theoretical mass flow rate variations for Modele: a) HPP, b) INJ, c) PCV, d) Leakage. Discontinuous lines suggest the time variation of these curves [27].

The prediction model can be expressed schematically as in fig. 4

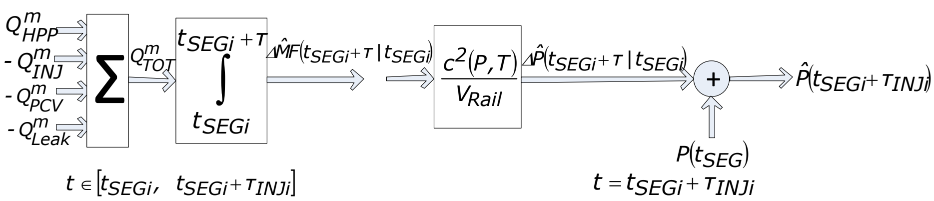

Figure 4. Schematic representation of CR pressure prediction analytical model

3 THEORETICAL SUPORT FOR MODELING AND IDENTIFICATION

In this chapter the theoretical background of the identification methodes further used in the application ephasizing on the capacity of Neuro – Fuzzy networks to incorporate *apriori* knlowlegde of the process and derive a numerical model out of process measured data is presented. The LOLIMOT [29] architecture and the input space partitioning algorithm are presented briefly. For model parameters optimization, the RLS method is proposed to be suitable for real time implementation.

The structure of a LOLIMOT type of model (fig. 5) contains M processing units, in particular M neurons. Each neuron implements a local linear model as:

$$\hat{y}_i = f_i \begin{pmatrix} u_1(k-1), \dots, u_1(k-n_{u_1}), \dots, u_p(k-1), \dots, u_p(k-n_{u_p}), \\ y_i(k-1), \dots, y_i(k-n_{y_i}) \end{pmatrix}, \quad i = 1, \cdots, M$$

which participates in an additive manner to the overall output $\hat{y}$. The local output $\hat{y}_i$ is weighted by the validity function Φ_i.

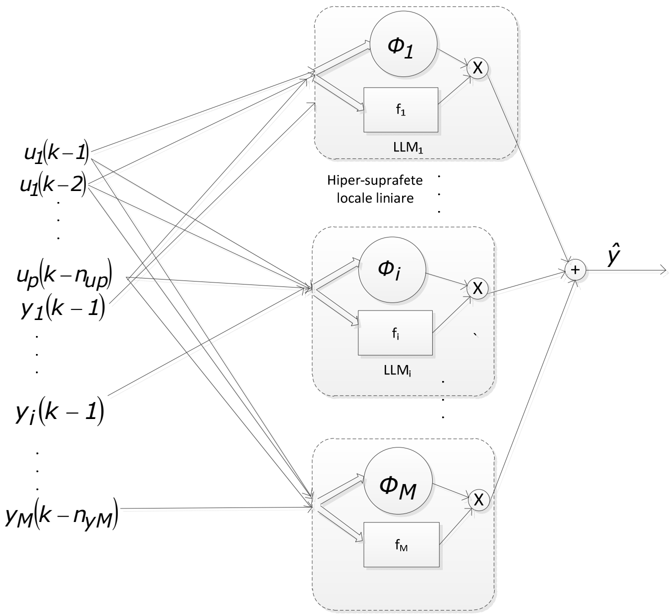

Figure 5. NARX implementation using LOLIMOT architecture

4 NEURO-FUZZY ADAPTIVE PREDICTION MODEL FOR CR PRESSURE

Having already proposed the model type, now the focus is on tailoring a model architecture to fit the process. The Common Rail system works in quasi-periodical regimes for a complete engine cycle (2 engine revolutions) which can be correlated with the crankshaft position $a_{CRK} \in [0,720)$. Further development of the model will refer only to the working regimes where the PCV is closed. In this way, a clear separation between hydraulic events may be achieved. This is required due to the highly nonlinear characteristics of the process.

During one period, there a 7 types of hidraulic events, as described in fig. 6. For all types, mutual exclusive membership functions are associated:

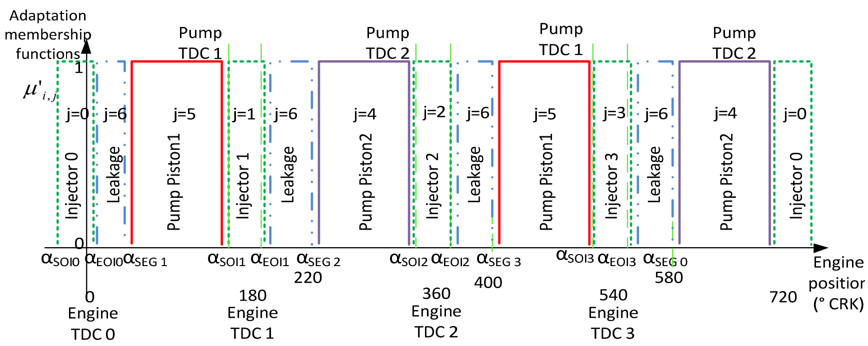

Figure 6. CR pressure phases and the associated membership functions [28].

The abovementioned events (j=0...6) are named *phases*. The computational marks on fig. 6 are called segment events ($\alpha_{i,SEGs+1} = \alpha_{i,SEGs} + 180°$) and they mark the start of prediction horizon while the middle value between start and end of an injection ($\alpha_{i,SOIs}, \alpha_{i,EOIs}$) marks the end of the prediction horizon.

CR pressure prediction model architecture consists in 2 levels: 1st level refers to Λ(T,P) input space, and 2nd level models the flow - pressure dynamics. In the top level, presented in fig. 7, the input of each linear model (LM) is $\underline{x}=[x_1, x_2, x_3]^T$, $\underline{z}=[z_1, z_2]^T$ and z', where: $x_1= Q^m_{HPP}$, $x_2= Q^m_{INJ}$, $x_3= Q^m_{Leak}$, $z_1=T$, $z_2=P$ şi $z'= \alpha_{CRK}$.

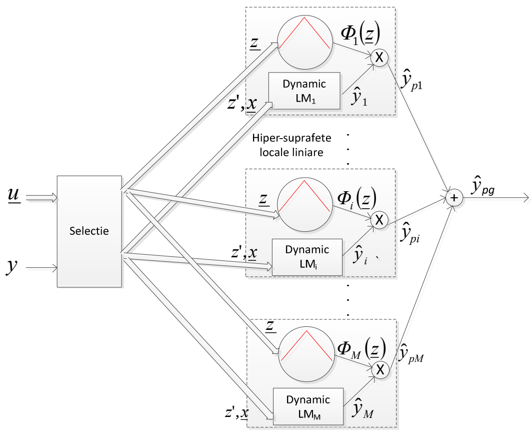

Figure 7. Neuro-Fuzzy network structure with local models [29]. The weight of each LM in the overall output is given by the triangular shaped validation functions Φ_i.

Each LM is, in fact, another Neuro – Fuzzy network on the 2nd level as described in fig. 8. A LM is formed out of 7 local linear models (LLMs) corresponding to each phase. The validity functions $\Phi'_{i,j}$ work as a disjoint operator allowing only one LLM at the time to be active. The LLMs model the pressure dynamics. They work as Hammerstein type of models with the nonlinear part represented by the flow rate curves and having 2nd order FIR filters for the linear part.

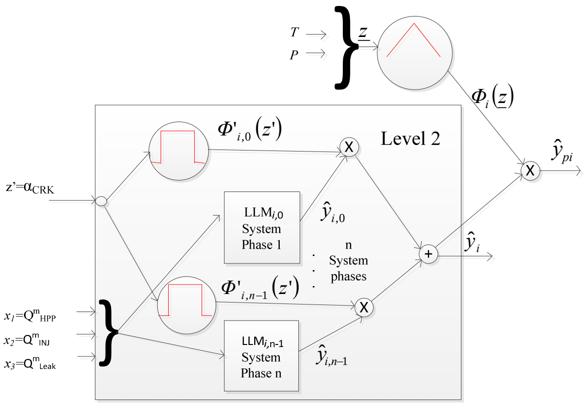

Figure 8. 2nd level Neuro-Fuzzy structure with LLMs [17].

The partitioning principle is provided by LOLIMOT [29] algorithm, which is nothing else, but a problem-solving algorithm based on "*divides et impera*". During one iteration, the workspace $S_{TP} = [T_{min}, T_{max}] \times [P_{min}, P_{max}]$ is refined by an axis orthogonal split on T or P axis which creates 2 new rectangular regions. The axis split decision is based on the evaluation of a quadratic cost function, which evaluates the quality of each local model associated with each rectangular region in S_{TP} :

$$I_{LMc_i/cm}\left(\bigcup_{j,l} w_{i,j,l}\right) = \frac{1}{N_V}\sum_{k=1}^{N_V} e_i^2(k), \quad e_i(k) = y(k) - \hat{y}_{LMc_i}(k).$$

Overall, we distinguish 2 work stages:

- Stage I: Creation of the Neuro-Fuzzy model structure. This stage is finalized with the determination of LM_1, .., LM_M and their corresponding membership functions.
- Stage II: *On–line* usage of the resulted model with continuous adaptation of coefficients.

According to the model architecture from fig. 8, each $LLM_{i,j}$ provides a value calculated with the formula:

$$\hat{y}_{i,j}(k) = \sum_{l=1}^{n_x} \underbrace{b_{i,j,l}(q^{-1})\, x_l(k)}_{\hat{y}_{i,j,l}(k)}, \quad b_{i,j,l}(q^{-1}) = b_{i,j,l}^1 q^{-1} + b_{i,j,l}^2 q^{-2}.$$

The model output at level 1 (fig. 7) is provided by the equation:

$$\Delta\hat{P}(k) = \hat{y}(k) = \sum_{i=1}^{M} \hat{y}_i(k)\Phi_i .$$

Since the model architecture is designed for complementation on a real-time ECU, the classical LOLIMOT structure with Gaussian membership functions was replaced by a structure with triangular shaped membership functions (fig. 9) exhibiting the prediction as the bilinear interpolation look-up tabels:

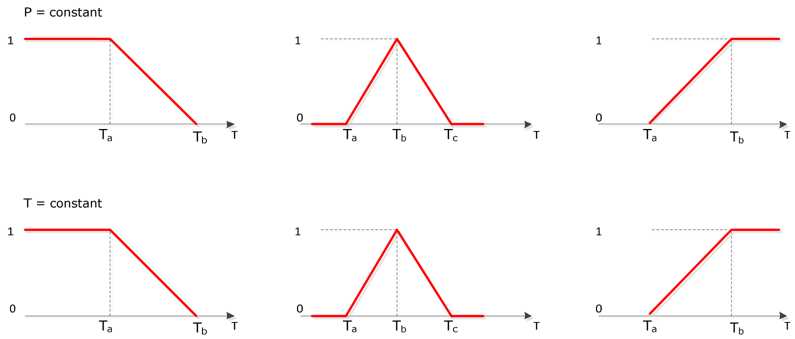

Figure 9. Triangular and trapezoidal shaped membership functions replacing the Gaussian type of functions.

5 SOFTWARE IMPLEMENTATION OF THE ADAPTIVE PREDICTION MODEL FOR CR PRESSURE

This chapter is dedicated to the usage of theoretical tools in solving a real world problem and presents the software implementation, optimized for a real time environment, of the proposed model architecture.

The first part of the chapter, treats some aspects related to the capabilities and restrictions imposed by the real time computation environment and the development of software solution. The Neuro-Fuzzy model with triangular shaped validity functions is converted to a more computational efficient model with look-up tables performing bilinear interpolation (fig. 10). A proof of the results similarity for the two solutions is provided.

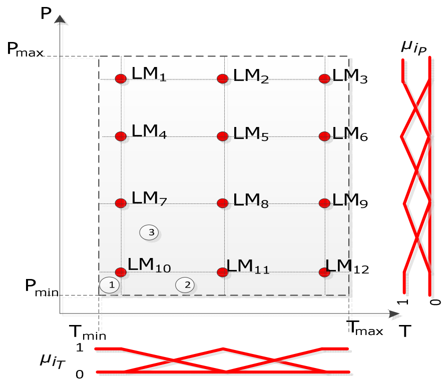

Figure 10. Positions of the working point Λ(P,T) with respect to a grid like break-point structure. On the outside, the corresponding validity functions were displayed.

The second part of the chapter describes the experimental environment while the last part studies the RLS algorithm as a closed loop system with discrete states. Some adjustments are performed to the original version of the algorithm increasing robustness against measurement noise and weak input excitation and ensuring convergence. The algorithm, presented as a discrete state model, can be also seen as a switching system (fig. 11).

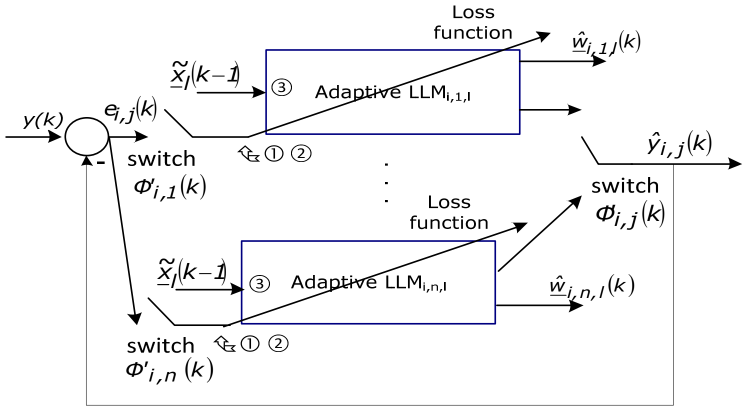

Figure 11. Adaptive structure seen as a switching system.

The modifications referred at points ①, ② and ③ have the objective of ensuring model coefficients convergence by reducing the RLS algorithm’s sensitivity to noise and robustness to weak input excitation. The enhanced algorithm is represented by the equation system:

$$
\begin{cases}
\begin{cases}
\underline{\hat{w}}_{i,j,l}(k+1) = \begin{cases} [I - \underline{\gamma}_{i,j,l}(k) \cdot \underline{\tilde{x}}_l^T(k)] \cdot \underline{\hat{w}}_{i,j,l}(k) + \underline{\gamma}_{i,j,l}(k) \cdot y(k), \; if \begin{cases} \Phi'_{i,j}(z'(k)) = 1 \\ |e_{i,j}(k)| \geq \delta \end{cases} \\ \underline{\hat{w}}_{i,j,l}(k), \; if \begin{cases} \Phi'_{i,j}(z'(k)) = 0 \\ |e_{i,j}(k)| < \delta \end{cases} \end{cases} & , \underline{\hat{w}}_{i,j,l}(0) = \underline{\hat{w}}_{i,j,l,0} \\
\underline{R}_{i,j,l}(k+1) = \begin{cases} \frac{1}{\lambda_i} [\underline{I} - \underline{\gamma}_{i,j,l}(k) \underline{\tilde{x}}_l^T(k)] \cdot \underline{R}_{i,j,l}(k), \; if \begin{cases} \Phi'_{i,j}(z'(k)) = 1 \\ \left|\underline{\tilde{x}}_l^T(k)\right| \geq \varepsilon \end{cases} \\ \underline{R}_{i,j,l}(k), \; if \begin{cases} \Phi'_{i,j}(z'(k)) = 0 \\ \left|\underline{\tilde{x}}_l^T(k)\right| < \varepsilon \end{cases} \end{cases} & , \underline{R}_{i,j,l}(0) = \underline{R}_{i,j,l,0}
\end{cases} \\
cu \\
\qquad \begin{cases} e_{i,j}(k) = \frac{1}{N_a} \sum_{i=k-N_a+1}^{k} \left(y(i) - \underline{\tilde{x}}_l^T(i) \cdot \underline{\hat{w}}_{i,j,l}(i) \right) \\ \gamma_{i,j,l}(k) = \frac{1}{\underline{\tilde{x}}_l^T(k) R_{i,j,l}(k) \underline{\tilde{x}}_l(k) + \lambda_i} \underline{R}_{i,j,l}(k) \cdot \underline{\tilde{x}}_l^T(k) \cdot \Phi_i(z(k)) \cdot \Phi'_{i,j}(z'(k)) \end{cases} \\
\underline{\hat{w}}_{i,j,l}(k) = [I_2 \quad 0] \cdot \begin{bmatrix} \underline{\hat{w}}_{i,j,l}(k) \\ \underline{R}_{i,j,l}(k) \end{bmatrix}
\end{cases}
$$

6 EXPERIMENTAL RESULTS

This chapter presents, systematically, the results of the input space decomposition algorithm (chapter 4) using the robust RLS algorithm (chapter 5). The performances of the model are evaluated and compared to the current solution. Finally, a solution optimized for real time implementation is proposed.

The final decomposition result is presented in fig. 12:

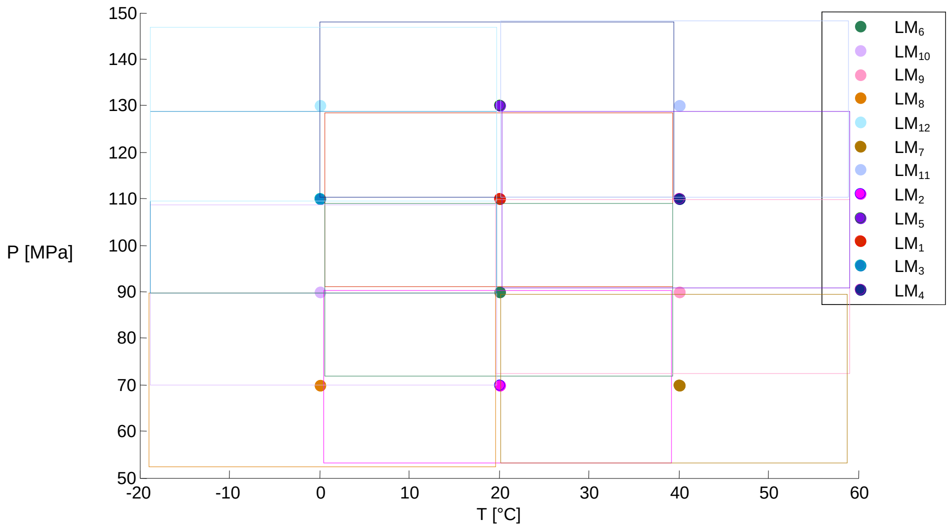

Figure 12. Axis orthogonal decomposition of input space in linear regions

Having the model structure determined and the coefficients identified, the next task was to validate the CR prediction model in a dynamic environment.

In figures 13 and 14 there is a comparative display of measured pressure with 1 ms recurrence (green), current solution: average pressure for previous segment *j*-1 (blue), calculated a time t_{SEGj} and predicted pressure for an interval equal to $[t_{SEGj}, 0.5(t_{SOIj+1} + t_{EOIj+1})]$. Figure 14 highlights using the triplets (A_1, A_2, A), (B_1,B_2,B), (C_1,C_2,C) and (D_1,D_2,D) the prediction model performance over the current solution in a dynamic pressure working point scenario, similar to the real situation. During injection, the real CR pressure value is A, while the value used for calculating the injection duration is A_1. The model predicted value in A_2, which is much closer to the measured value. For points B, C and D similar results holds.

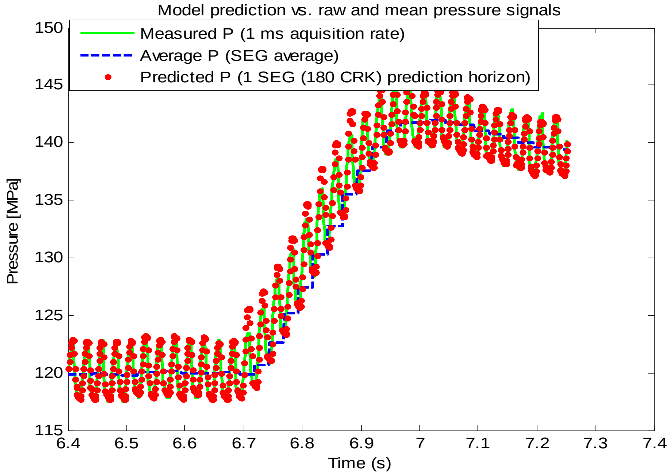

Figure 13. Measured pressure (1 ms) - red, last segment average - blue and predicted value – green for an ascending pressure setpoint.

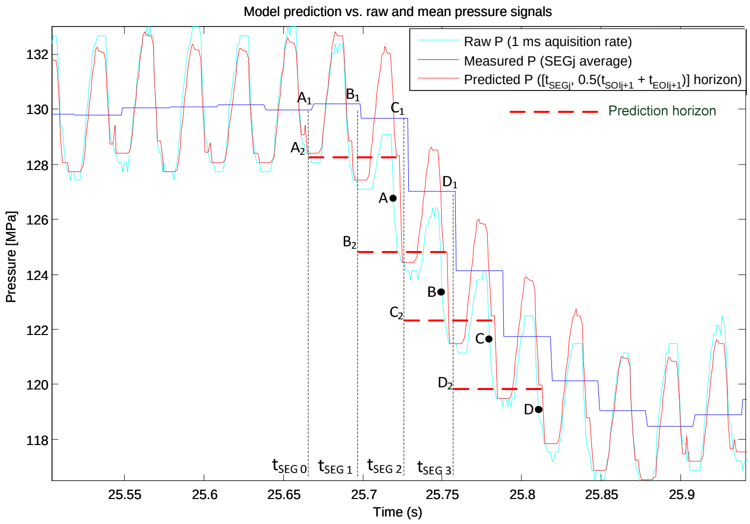

Figure 14. Measured pressure (1 ms) - red, last segment average - blue and predicted value – light blue for a descending pressure setpoint.

From RIP (Rule based InterPolation) [57, 66] method perspective, the entire prediction model can be displayed in a look-up table with bilinear interpolation (Table I)

TABEL I. RULE BASE ASOCIATED WITH THE EXPERIMENTAL MODEL

	LM			
Low temperature	LM_8	LM_{10}	LM_3	LM_{12}
Medium temperature	LM_2	LM_6	LM_1	LM_5
High temperature	LM_7	LM_9	LM_4	LM_{11}
T / P	Low Pressure	Moderate pressure	Medium Pressure	High Pressure

A more convenient way to represent the coefficients is using 2D graphics of different temperature characteristic curves. E.g., in fig. 15, the coefficient $w^{1}_{i,j,l}(P)$ for pump piston 1 is represented as a function of parameter T = 0 ^{0}C, 20 ^{0}C and 40 ^{0}C :

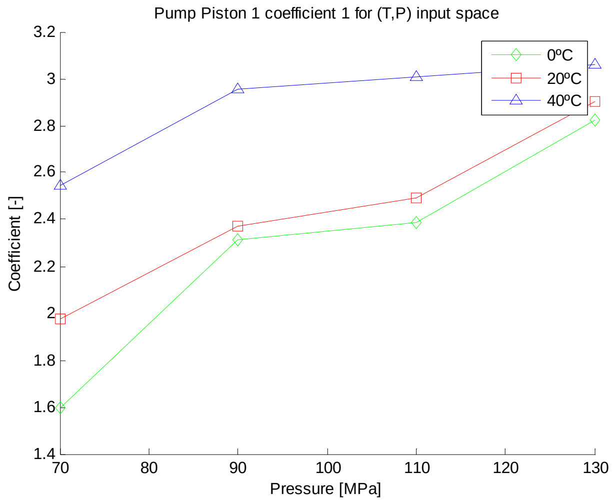

Figure 15. Coefficient characteristic curves $w^{1}_{i,4,1}(P), T = const.$ (Pump piston 1).

7 CONCLUSIONS, CONTRIBUTIONS AND PERSPECTIVES

The PhD thesis has achieved the main goal of developing a neuro-fuzzy model implemented in a real time optimized application using interpolative look-up tables, designated for predicting the fuel pressure variations inside the common rail of a diesel engine.

From the applicative point of view, the thesis synthesizes the following contributions:

- Synthesis of a neuro-fuzzy type of structure for identification and prediction of common-rail pressure.
- Real time implementation of the prediction model on a Tricore CPU using OSEK –VDA operating system.
- Validation of the prediction model on the experimental hydraulic test-bench for a wide range of the input space.

The scientific and theoretical contributions are:

- Determination of an analytical flow – pressure model for predicting the common – rail system pressure variation using mass conservation principle.
- Application of neuro-fuzzy modeling theory for realizing a structure with local linear models used for common-rail pressure dynamics identification
- Optimization of the resulted neuro-fuzzy structure for implementation on a real time system.
- Tailoring of LOLIMOT algorithm for a faster determination of linear regions.

• A new robust RLS algorithm is proposed suitable for usage in a real time environment. The main features are robustness to weak input excitation and systematic noise rejection.

The intermediate results of the research have been valorized in papers published by the author:

- Ioanas, G.L., „Modeling, Identification and Prediction of Inherent quasi-stationary Pressure Dynamics of a Common-Rail System using Neuro-Fuzzy Structures with Local Linear ARX models”, Control Engineering and Applied Informatics Journal, Bucuresti, Romania, Vol. 14, no.3, pp. 61-70, 2012.
- Ioanas, G.L, Dragomir, T.L., „Common-rail Pressure Estimation using a Neuro- Fuzzy architecture with Local Hammerstein Models”, Proc. of SACII 2013, IEEE 8th International Symposium on Applied Computational Intelligence and Informatics, Timişoara, pp. 281-286, 2013.
- Ioanas, G.L., Dragomir, T.L., „Local linear models adaptation for a 4 Inj – 2PP Commonrail Pressure System”, IEEE 11th International Symposium on Intelligent Systems and Informatics, SISY 2013, Subotica, pp. 253-258, 2013.
- Ioanas, G.L., Dragomir, T.L., „Dynamic models adaptation for a 4 Inj – 2PP Commonrail Pressure System”, 39th Annual Conference of the IEEE Industrial Electronics Society IECON 2013, Viena, pp. 3490 – 3495, 2013.

Considering the practical perspectives of this research we ca say that the common-rail pressure prediction model can be adapted for industrialization in the automotive industry. Furthermore, other nonlinear processes may be modeled and identified using the methodology presented in this paper.

The author is indebted to Continental Powertrain Engine Systems for the generous technical support and address many thanks.

This work was partially supported by the strategic grant POSDRU/88/1.5/S/50783, Project ID50783 (2009), co-financed by the European Social Fund – Investing in People, within the Sectorial Operational Program Human Resources Development 2007 – 2013.

SELECTIVE BIBLIOGRAPHY

[1] Hafner, M., Schuler, M. and Nelles, O., „Neural net models for diesel engines-simulation and exhaust optimization”, Control Engineering Practice, Vol. 30, No. 2, pp. 402-412, 2002.

[2] R. Isermann O. Nelles, A. Fink, „Local linear model trees (lolimot) toolbox for nonlinear system identification”, 12th IFAC Symposium on System Identification, (SYSID), Santa Barbara, USA, 2000.

[3] Jakubek S., Keuth N. „A local neuro-fuzzy network for high-dimensional models and optimization”. Engineering Applications of Artificial Intelligence 19 705–717, 2006.

[4] Froehlich M., “Informationstheoretische Optimierung kunstlicher neuronaler Netze fur den Einsatz în Steuergeraten”, *PhD thesis at Eberhard-Karls University of Tubingen*, 2003.

[5] https://www.avl.com/c/document_library/get_file?uuid=56fe5fc4-3e6d-4f9e-93a9-dd419b026fea&groupId=10138. Accesat în 30.08.2013.

[6] http://www.dieselnet.com/standards/eu/ld.php. Accesat în 30.08.2013.

[7] http://www.dieselnet.com/standards/us/ld_ca.php. Accesat în 30.08.2013.

[8] Bosch, R. GmbH, Diesel-Engine Management, 3rd edition, Automotive Technology, 2004.

[9] Liu, Y, Zhang, Y., Qiu, T. *et al.* , „Optimization research for a high pressure common rail diesel engine based on simulation”, International Journal of Automotive Technology, Volume 11, Issue 5, pp 625-636, October 2010.

[10] Borchsenius, F., Stegemann, D., Gebhardt, X. *et al.*, „Simulation of diesel common rail injection systems”, MTZ worldwide, Volume 71, Issue 6, pp 42-45, 2010.

[11] Catania A. E., Ferrari A., Manno M., „Development and Application of a Complete Multijet Common-Rail Injection-System Mathematical Model for Hydrodynamic Analysis and Diagnostics‟, *Trans.-Asme Journal of Engineering for Gas Turbines and Power*; 130, 6; 062809, American Society of Mechanical Engineers, 2008.

[12] Catania A. E., Ferrari A., Spessa E., „Numerical-Experimental Study and Solutions to Reduce The Dwell Time Threshold for Fusion-Free Consecutive Injections în a Multijet Solenoid-Type CR System [1]‟, *Journal of Engineering for Gas Turbines and Power*, Vol. 131, Issue 2, Dec 2008.

[13] Catania A. E., Ferrari A., Manno M., Spessa E., „Experimental Investigation of Dynamics Effects on Multiple-Injection Common Rail System Performance”, *Journal of Engineering for Gas Turbines and Power-transactions of The Asme* 01/2008.

[14] Wang T. C., Schwarz E., Bryzik W., Han J. S., Xie X. B., Lai M. C., Henein N. A., „Parametric Characterization of High-Pressure Diesel Fuel Injection Systems”, Journal of Engineering for Gas Turbines and Power, Vol. 125, Issue 2, Apr 29, 2003.

[15] Baratta M., Catania A. E., Ferrari A., „Hydraulic Circuit Design Rules to remove the Dependence of the Injected Fuel Amount on Dwell Time în Multijet CR Systems‟, *Journal of Fluids Engineering*, Vol. 130, Issue 12, 27 Oct 2008.

[16] Gauthier C., Sename O., Dugard L., Meissonnier G., „Modelling of a Diesel Engine Common Rail Injection System‟, *Proceedings of the 16th IFAC World Congress*, Vol. 16, Part 1, Czech Republic, 2005.

[17] **Ioanas, G.L**., Dragomir, T.L., „Common-rail Pressure Estimation using a Neuro-Fuzzy architecture with Local Hammerstein Models”, Proc. of SACII 2013, IEEE 8th International Symposium on Applied Computational Intelligence and Informatics, pp. 281-286, 2013.

[18] Lino P., Maione B., Rizzo A., „Nonlinear Modelling and Control of a Common Rail Injection System for Diesel Engines‟, *Applied Mathematical Modelling* 31 (2007) 1770-1784.

[19] Lino P., Maione B., Amorese C., „Modelling and Predictive Control of a New Injection System for Compressed Natural Gas Engines‟, *Control Engineering Practice 16* (2008) 1216-1230.

[20] Li, Z., „Condition Monitoring of Axial Piston Pump‟, Thesis for the Degree of Master of Science în the Department of Mechanical Engineering University of Saskatchewan, Saskatoon, Canada,November 2005.

[21] Seykens, X.J.L., Somers, L.M.T. & Baert, R.S.G . Modeling of common rail fuel injection system and influence of fluid properties on injection process. Proceedings of VAFSEP, Dublin, Ireland, 2004.

[22] Boudy, F., Seers, P. „Impact of physical properties of biodiesel on the injection process în a common-rail direct injection system”, Energy Conversion and Management 50, p. 2905 – 2912, 2009.

[23] Kiijarvi, J., „Diesel fuel injection system simulation”, Publications of the Internal Combustion Engine Laboratory, Helsinki University of Technology, No. 77, pp. 126, 2003.

[24] Zhang Z., Sun Z., „Rotational Angle Based Pressure Control of a Common Rail Fuel Injection System for Internal Combustion Engines”, American Control Conference Hyatt Regency Riverfront, St. Louis, MO, USA, 2009.

[25] Schaschke, C., Fletcher, I. and Glen, N., "Density and Viscosity Measurement of Diesel Fuels at Combined High Pressure and Elevated Temperature”, Processes 2013, 1, 30-48.

[26] **Ioanas, G.L.**, „Modeling, Identification and Prediction of Inherent quasi-stationary Pressure Dynamics of a Common-Rail System using Neuro-Fuzzy Structures with Local Linear ARX models”, Control Engineering and Applied Informatics Journal, Bucuresti, Romania, Vol. 14, no.3, pp. 61-70, 2012.

[27] **Ioanas, G.L.**, Dragomir, T.L., „Local linear models adaptation for a 4 Inj – 2PP Commonrail Pressure System”, IEEE 11th International Symposium on Intelligent Systems and Informatics, SISY 2013, Subotica, pp. 253 – 258, 2013.

[28] **Ioanas, G.L.**, Dragomir, T.L., „Dynamic models adaptation for a 4 Inj – 2PP Commonrail Pressure System”, 39th Annual Conference of the IEEE Industrial Electronics Society, IECON 2013, Viena, pp. 3490 – 3495, 2013.

[29] Nelles, O., Nonlinear System Identification, Springer- Verlag, cap. 11, 13, 14, 19, 20, 21, 23, 2001.